Shape of Fluid Vesicles Anchored by Rigid Rod

Mingzhu Sun, Feng Qiu, Hongdong Zhang, and Yuliang Yang*

Department of Macromolecular Science, The Key Laboratory of Molecular Engineering of Polymers, Ministry of Education, China, Fudan University, Shanghai, 200433 China

Received: October 31, 2005; In Final Form: March 2, 2006

A method combined the self-consistent field theory (SCFT) for the rigid rod with the Helfrich curvature elasticity theory for the vesicle has been developed for studying the shape of vesicles anchored by rigid rod. Both the deformation of the vesicle and the density distribution of rod segments can be obtained. Because of the vesicle's impenetrability for the rod segments and the decrease of the available space for the rod orientational configurations, the anchored rod segments exert the inhomogeneous entropic pressure on the vesicle and induce the change of vesicle shape. The interaction between the rod segments and the vesicle membrane exerts an extra tension to the membrane. Thus the interaction between the vesicle membrane and the rod segments, the rod length, and the bending rigidity of vesicle are investigated as the important factors to the shape transformation of the vesicle and the density distribution of rod segments. This method can be extended to more complicated and real biological systems, such as polymers with different topological architectures/vesicle, multiple chains/vesicle, protein inclusions, etc.

1. Introduction

Membranes and vesicles anchored by polymers provide simple model systems of biological membranes such as the plasma membrane of the cell. These biological and biomimetic membranes consist of a lipid bilayer. The extracellular part of the cell membrane is decorated by glycolipids and glycoproteins, which protect the cell against mechanical and chemical attack.[1,2] These "ornaments" are usually semiflexible or even rigid macromolecules. The process of budding and fission of cell are plausibly induced by these proteins. As a simple model of biological membranes, in recent years, tremendous interest has been focused on the polymer anchored vesicles. Numerous experiments have been carried out on the system of polymer chain anchored fluid vesicles, and some bio-related processes have been observed such as budding, increnation, pearling, tubulation, coiling, etc.[3,4]

Polymers can usually be anchored onto membranes by two kinds of methods: one is by a lipid anchor that is covalently bound to a water-soluble polymer; the other is by hydrophobic side groups of the polymer which sticks onto the bilayer with physical interaction. For one anchored polymer chain, its overall loss of conformation entropy arising from the impenetrable membrane surface is only a few k_BT, which is less than the anchoring energy ($\sim 20\ k_BT$), thus this anchored course can be easily achieved. For this reason, this kinds of biomimetic system can be easily investigated.[5,6]

There are many theoretical methods that have been devoted to study the subtle shape changes of the polymer chains/membrane compound system, such as theoretical analysis or Monte Carlo simulations.[7−16] Their results revealed that the chain anchoring can induce local inhomogeneity of the bending rigidity and spontaneous curvature of the membrane. In reality, when the polymer chain comes close to the membrane, the conformational entropy of the polymer is reduced due to the restriction of the available activity space, the anchored chain segments exert an inhomogeneous entropic pressure on the vesicle, and the shape of membrane is transformed. Unfortunately, these models ignored the fact that the polymer chain could also affect the tension of membrane via the adsorption or repulsion interaction between polymer segment and membrane, and the membrane tension is also known as partly suppressing or aggrandizing the membrane shape fluctuation. In addition, most of theoretical studies are limited to the case of flexible polymer chains anchored on a flat membrane of infinite size. However, for vesicles, due to the closure of the membranes, additional effects not present in planar membranes show up. Therefore, the theories developed for planar membrane can hardly be used to interpret the experimental results on the shape transformation of vesicles of finite sized and closed membrane.

Recently, we have developed a method that combines self-consistent-field theory (SCFT) for Gaussian chain and Helfrich curvature elasticity theory for fluid membrane to determine the stable and metastable shapes of flexible chain anchored vesicle.[17] However, for many real cell membranes, the "ornaments" that anchored on the membrane usually are semiflexible or even rigid macromolecules. Therefore, we believe that the system of rod-anchored vesicle has more biological relevance. Although, the theoretical method developed previously[17] has also been extended to investigate the deformation of a rod-anchored flat membrane of infinite size,[18] the behaviors of rod-anchored vesicle still need to be explored.

In this paper, we would like to extend the method developed previously[17] to the case of rod-anchored vesicle and explore in detail the rod anchoring induced shape deformation of vesicle. The paper is organized as follows. In the next section, the model and algorithm for studying the system of rod-anchored vesicle will be introduced. In section 3, the effects of interaction strength between the vesicle and the rod, the rod length, the surface tension, and the bending rigidity of the membrane on the vesicle shapes are discussed based on the calculated results. In the last section, we draw conclusions and make some remarks.

* Corresponding author. E-mail: ylyang@fudan.ac.cn.

10.1021/jp0562633 CCC: $33.50
Published on Web 04/21/2006

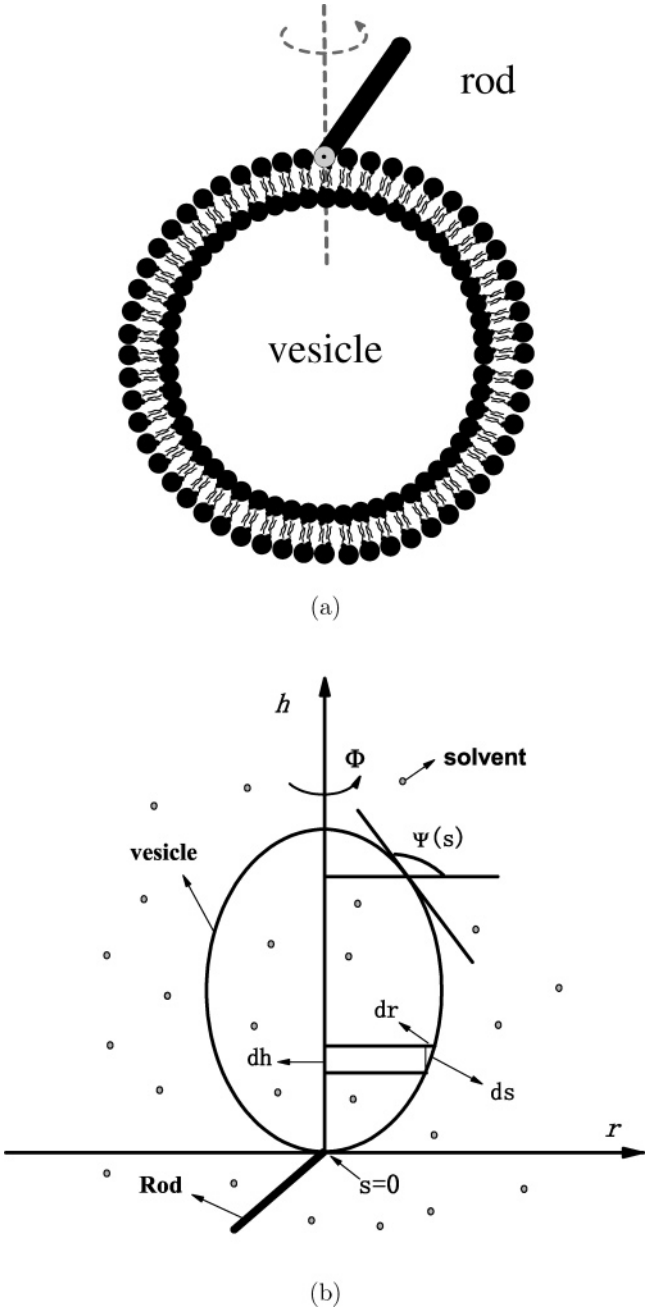

Figure 1. Schematic illustration of one end of a rigid rod with length $N_p b$ anchored on an vesicle at ($r = 0$, $h(r) = 0$). (a) 2D illustration, (b) 2D coordinate. The vesicle height at r is $h(r)$. Φ is the azimuthal angle, and Ψ is the angle between the tangent to the contour and the r axis.

2. Model and Algorithm

The model of a single rod-anchored vesicle is schematically drawn in Figure 1. We assume that the rod can freely rotate around the pintle at one end of the rod. In the system, there are n_s solvent molecules and a rigid rod with one end anchored to outside or inside vesicle wall. The rod consists of N_p segments of length b. The diameter of the rod and the size of the solvent are also taken to be the unit length b. In general, the thickness of the lipid bilayer is about 4 nm, and the lateral size can extend up to the μm range. It is therefore justified to neglect the thickness and to model the vesicle membrane mesoscopically as a two-dimensional elastic surface. We assume that the membrane is impenetrable to the rod segments. The system is assumed to be homogeneous and incompressible with the reference density ρ_0. Defining the solvent density operator as $\hat{\rho}_s(r) = \sum_{i=1}^{n_s}\delta[r - \mathbf{R}_s^i]$, rod density operator as $\hat{\rho}_p(r) = \int_0^{N_p} d\tau\delta(r - \mathbf{R}_p(\tau)) = \int d\mathbf{n}_\mathbf{R} \int_0^{N_p} d\tau\delta(r - \tau\mathbf{n}_\mathbf{R} - \mathbf{R}_m(0, 0))$, where $\mathbf{n}_\mathbf{R}$ is a unit vector along the rod axes that can be written as $\mathbf{n}_\mathbf{R}(\phi, \theta)$ ($\phi \in [0, 2\pi)$ and $\theta \in [0, \pi)$). It implies that the rod can freely rotate around the anchored pivot. The partition function of such a system can be written as

$$\Xi = \mathcal{N}\frac{1}{n_s!}\int\prod_{i=1}^{n_s} D\mathbf{R}_s^i \int D\mathbf{R}_p(\tau)e^{-\beta H_p^0[\mathbf{R}_p(\tau)]} \int D\mathbf{R}_m(u, v)e^{-\beta H_m^0[\mathbf{R}_m(u,v)]}e^{-\beta H_{int}} \prod_r \delta[\hat{\rho}_p(r) + \hat{\rho}_s(r) - \rho_0]\delta(\mathbf{R}_m(0, 0) - \mathbf{R}_p(0))\delta\left[\int_{r\in V_{in}[\mathbf{R}_m(u, v)]} dr\hat{\rho}_p(r)\right] \quad (1)$$

where $\mathcal{N}$ is a constant, $\beta = 1/k_BT$, and $\int D\mathbf{R}$ denotes functional integration over all the configurations of solvents, rod, and fluid membrane. $\mathbf{R}_s^i$ and $\mathbf{R}_p(\tau)$ denote the spatial positions of the solvent molecule i and the segment τ of the rigid rod, respectively. $\mathbf{R}_m(u, v)$ denotes the spatial position of the membrane and u, v are curvilinear coordinates in the membrane surface. $r \in V_{in}[\mathbf{R}_m(u, v)]$ or $r \in V_{out}[\mathbf{R}_m(u, v)]$ denotes that r is inside or outside the volume enclosed by the vesicle membrane, respectively. The first δ-function ensures the incompressibility constraint, and the third δ-function guarantees that the membrane is impenetrable by rod. H_{int} denotes the interaction Hamiltonian which includes interactions between the rod segments and solvent molecules and the membrane, etc. Hence, $H_{int} = V_{ps} + V_{pm} + V_{sm}$, which can be written as $\beta V_{ps} = \chi \int dr\hat{\rho}_p(r)\hat{\rho}_s(r)$ for rod/solvent, $\beta V_{pm} = \nu \oint dA\hat{\rho}_p(r \in A[\mathbf{R}_m(u, v)])$ for rod/membrane and $\beta V_{sm} = \mu \oint dA\hat{\rho}_s(r \in A[\mathbf{R}_m(u, v)])$, where χ and ν, μ are the Flory−Huggins interaction parameters of rod/solvent, rod/membrane, and solvent/membrane pairs, respectively. $A[\mathbf{R}_m(u, v)]$ represents the surface of the closed vesicle membrane. The Hamiltonian of the semiflexible polymer can be written as[19]

$$H_p^0[\mathbf{R}_p] = \frac{3}{2b^2}\int_0^{N_p} d\tau\left[\frac{\partial\mathbf{R}_p(\tau)}{\partial\tau}\right]^2 + \frac{l_p}{2}\int_0^{N_p} d\tau\left[\frac{\partial^2\mathbf{R}_p(\tau)}{\partial\tau^2}\right]^2 \quad (2)$$

where l_p is the persistent length, and $\partial^2\mathbf{R}_p(\tau)/\partial\tau^2$ is the local curvature of the semiflexible chain. A rigid rod is the limit configuration of semiflexible chain. For a rigid rod, $\partial\mathbf{R}_p(\tau)/\partial\tau$ is a constant, and $\partial^2\mathbf{R}_p(\tau)/\partial\tau^2 = 0$ and its persistent length $l_p \gg N_p b$.[19,20] It is reasonable to assume $H_p^0[\mathbf{R}_p(\tau)] =$ constant. The Hamiltonian of the vesicle has been proposed by Ou-Yang and Helfrich:[21]

$$\beta H_m^0[\mathbf{R}_m] = \frac{\kappa}{2}\oint_{A\in\mathbf{R}_m(u,v)} dA(2H + c_0)^2 + \lambda\oint_{A\in\mathbf{R}_m(u,v)} dA + \Delta p\int_{r\in V_{in}[\mathbf{R}_m(u,v)]} dr \quad (3)$$

where H and c_0 are the local mean curvature and spontaneous curvature of the fluid membrane, respectively. κ is the bending rigidity of the membrane, λ can be considered as the tensile stress acting on the membrane, and $\Delta p = p_{out} - p_{in}$ is the pressure difference across the membrane.

Following the standard procedure of the SCFT,[22] by introducing external auxiliary fields ω_p and ω_s, which are the self-consistent molecular fields conjugated to the collective densities ρ_p and ρ_s, and the Lagrangian multipliers ξ for the incompressibility of the system as well as ζ for the impenetrability of the

membrane, thus eq 1 can be rewritten as

$$\Xi = \int \mathcal{D}\mathbf{R}_m \int \mathcal{D}\rho_p \int \mathcal{D}\omega_p \int \mathcal{D}\rho_s \int \mathcal{D}\omega_s \int \mathcal{D}\xi \int \mathcal{D}\zeta e^{-\beta\mathcal{F}\{\mathbf{R}_m,\rho_s,\rho_p,\omega_s,\omega_p,\xi,\zeta\}} \quad (4)$$

with the free energy functional βF defined as

$$\beta\mathcal{F} = -\ln Q_p[\omega_p] - n_s \ln Q_s[\omega_s] + \int dr[\chi\rho_s\rho_p - \omega_s\rho_s - \omega_p\rho_p + \xi(\rho_p + \rho_s - \rho_0)] + \frac{\kappa}{2}\oint_{A\in\mathbf{R}_m(u,v)} dA(2H + c_0)^2 + \lambda\oint_{A\in\mathbf{R}_m(u,v)} dA + \Delta p \int_{r\in V_{in}[\mathbf{R}_m]} dr + \eta\oint_{A\in\mathbf{R}_m(u,v)} dA\rho_p + \zeta \int_{r\in V_{in}[\mathbf{R}_m]} dr\rho_p \quad (5)$$

where $\eta = \nu - \mu$. In eq 5, $Q_p\{\omega_p\}$ denotes the partition function of the single rod in the molecular field ω_p with one end anchored at point $\mathbf{R}_m(0, 0)$, $Q_s\{\omega_s\}$ is the partition function of solvent molecules treated as only one spherical segment in the molecular field ω_s. These partition functions can be expressed in the following forms:

$$Q_s\{\omega_s\} = \int d\mathbf{r} \exp\{-\omega_s(r)\} \quad (6)$$

$$Q_p\{\omega_p\} = \int \mathcal{D}\mathbf{R}_p \exp\{-\int_0^{N_p} d\tau\omega(\mathbf{R}_p(\tau))\}\delta(\mathbf{R}_p(0) - \mathbf{R}_m(0)) \quad (7)$$

The partition function Q_p for rigid rod can be easily obtained without solving the diffusion equation as Gaussian chain, similar to solvent molecules but to occupy N_p segments with spatial orientational dependence.

To obtain the stable or metastable state of the system, minimizing the free energy with respect to ρ_p, ρ_s, ω_p, ω_s, ξ, ζ, and results in the following self-consistent equations for the rod and solvents:

$$\omega_p(r) = \begin{cases} \eta/b + \chi\rho_s(r) + \xi(r) & r \in A[\mathbf{R}_m] \\ \zeta + \chi\rho_s(r) + \xi(r) & r \in V_{in}[\mathbf{R}_m] \\ \chi\rho_s(r) + \xi(r) & r \in V_{out}[\mathbf{R}_m] \end{cases} \quad (8)$$

$$\omega_s(r) = \chi\rho_p(r) + \xi(r) \quad (9)$$

$$\rho_p(r) = \frac{1}{Q_p}\exp\{-\int_0^{N_p} d\tau\omega_p(\mathbf{R}_p(\tau))\}\delta(r - \mathbf{R}_p(\tau)) \quad (10)$$

$$\rho_s(r) = \frac{n_s}{Q_s}\exp\{-\omega_s(r)\} \quad (11)$$

$$\rho_0 = \rho_p(r) + \rho_s(r) \quad (12)$$

$$0 = \int_{r\in V_{in}[\mathbf{R}_m]} dr\rho_p(r) \quad (13)$$

and following the standard procedure of the functional $\mathcal{F}$ minimization for fluid membranes,[23] we obtain the shape equation of the vesicle in the presence of rod:

$$\{\Delta p + \zeta\rho_p(r \in A[\mathbf{R}_m]) + \eta\mathbf{n}\cdot\nabla\rho_p(r \in A[\mathbf{R}_m])\} - 2H\{\lambda + \eta\rho_p(r \in A[\mathbf{R}_m])\} + 2\kappa\nabla^2 H + \kappa(2H + c_0)(2H^2 - c_0H - 2K) = 0 \quad (14)$$

where $\mathbf{n}\cdot\nabla\rho(r \in A[\mathbf{R}_m])$ denotes the concentration gradient of the rigid rod segments along the normal direction on the membrane $\mathbf{n}$, and K is the Gaussian curvature of the membrane.

Compared with the general shape equation of vesicles without rod anchoring, eq 15, derived by Ou-Yang and Helfrich:[21,23]

$$\Delta p - 2\lambda H + 2\kappa\nabla^2 H + \kappa(2H + c_0)(2H^2 - c_0H - 2K) = 0 \quad (15)$$

the physical implication of eq 14 is manifest. The extra pressure and tensile stress terms appear in eq 14, which is the same with the shape equation of the system of Gaussian chain-anchored vesicle.[17] The extra pressure $\zeta\rho_p(r \in A[\mathbf{R}_m])$ originates from the reduction of the rod conformation entropy due to the spatial confinement of the rod by the impenetrable vesicle membrane, and it can be named as inhomogeneous entropic pressure. This result coincides with the mean-field analysis by Bickel and Marques[16] for an impenetrable fluid membrane ornamented with grafted chain. The extra tensile stress $\eta\rho_p(r \in A[\mathbf{R}_m])$ comes from the interaction of the rod segments onto the vesicle membrane, which exerts extra inhomogeneous tensile stress acting on the membrane. This inhomogeneous tension term simply reflects that if the membrane adsorbs the chain, it reduces the tensile stress; thus, the membrane tends to be extended to decrease the free energy. In addition, the interaction of rod with the membrane also results in additional pressure $\eta\mathbf{n}\cdot\nabla\rho_p(r \in A[\mathbf{R}_m])$, which also reflects the membrane tends to contact more rod segments if it adsorbs rod segments.

As shown in Figure 1b, the shape equation can be solved by using the algorithm of Seifert et al. for an axial symmetric vesicle.[24] We use the arclength s along the contour and the azimuthal angle ϕ as coordinates. The shape is then determined by the tilt angle $\Psi(s)$, as defined in Figure 1b. Moreover the coordinates r and h are perpendicular and parallel to the axis of symmetry, respectively. In the numerical simulations, the box size is 5×20 with $\Delta h = 0.05$ and $\Delta r = 0.05$, and set $\Delta\tau = 0.05$ and $b = 0.05$. The numerical scheme we used is as follows. First we guess an initial vesicle shape (such as sphere), and then the self-consistent eqs 8−14 are solved to obtain $\rho_p(r, h)$. The obtained $\rho_p(r, h)$ is then inserted into eq 14 for calculating the new shape of the vesicle under the influence of the anchoring rod. These steps are repeated until the convergence conditions have been reached. Then the thermodynamic stable or metastable state for the system of rod-anchored vesicle is obtained. Throughout this paper, the solution of shape equation is obtained by comparing different energies of possible shapes, and the shape with local minima energy is selected to be the resulting one. In addition, because the surface area of vesicle will not change dramatically in the biological system and experiments, most of calculations are performed under fixed surface area. Given fixed surface area (A_0) of vesicle, search for the appropriate λ using successive over relaxation method and the iterative procedure ends with the additive constraint of $(A - A_0)/A_0$ meeting the convergence conditions. The rod and the vesicle both have their lengths scales in units of b and their energies scales in units of the bending constant k_BT, so all the parameters are dimensionless, and it can be transformed back to the real physical values: $\kappa \rightarrow \kappa k_BT$, $\lambda \rightarrow \lambda k_BT/b^2$, $\Delta p \rightarrow \Delta p k_BT/b^3$, $\eta \rightarrow \eta k_BT/b$, $\chi \rightarrow \chi k_BTb^3$, $\zeta \rightarrow \zeta k_BT$. Throughout this paper, the chosen parameters, $\lambda = 10^{-4}-10^{-2}k_BT/\text{nm}^2$, $\kappa = 1-25k_BT$, $\eta = -0.1$ to $0.1k_BT$, are all in the reasonable order of magnitude in real experiments.[23,25,26]

It should be noted that the justification for the self-consistent approximation is that a single chain encounters many more of its neighbors than itself and therefore exists in a mean field generated by the presence of its neighbors. In our system, SCFT

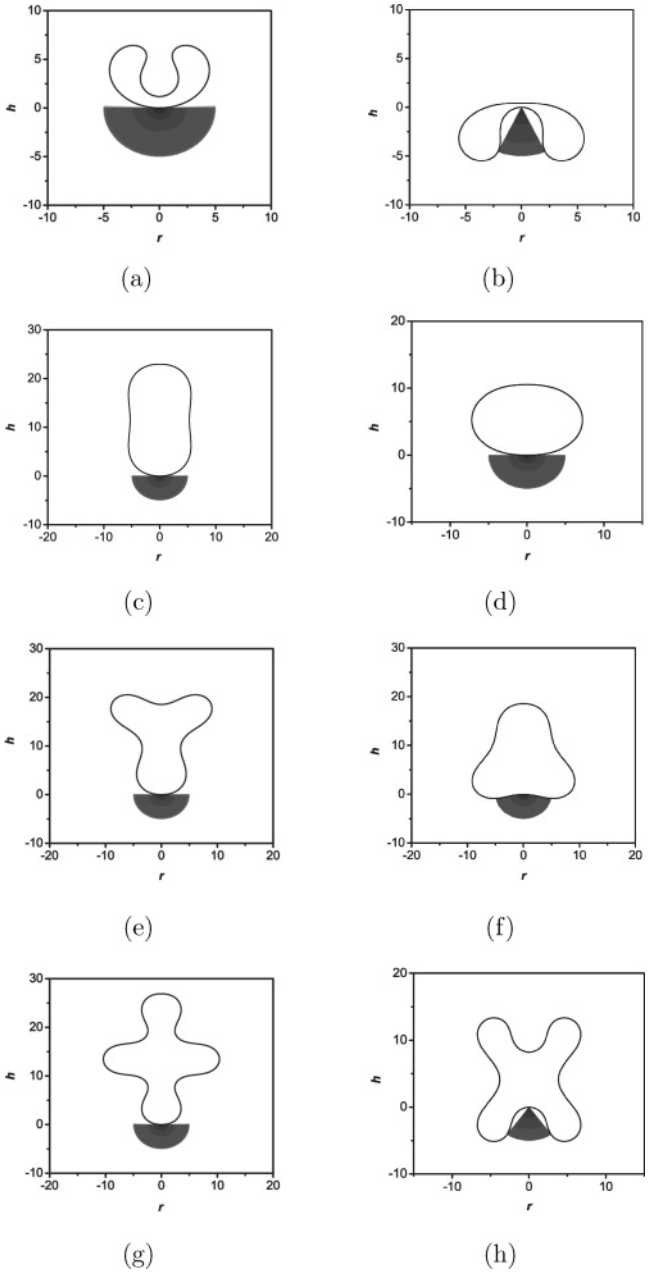

Figure 2. Typical stationary solutions of vesicle anchored by rigid rod outside, including shapes of the vesicle and segment distributions of the anchored rod. The shape of the vesicle is represented by the solid curve, and the density of the polymer chain is drawn in gray scale on a logarithmic scale. The radial (horizontal) and height axes are scaled by Nb. In all cases, we use $N_p = 100$, $c_0 = 0$, $\chi = 0$, $\eta = 0$. (a) $\kappa = 15$, $\Delta p = 0.0036$, $\lambda = -0.027$. (b) $\kappa = 10$, $\Delta p = 0.0024$, $\lambda = -0.02$. (c) $\kappa = 3$, $\Delta p = 0.00072$, $\lambda = -0.0132$. (d) $\kappa = 5$, $\Delta p = 0.0012$, $\lambda = -0.02$. (e) $\kappa = 2$, $\Delta p = 0.00048$, $\lambda = -0.008$. (f) $\kappa = 2$, $\Delta p = 0.00048$, $\lambda = -0.0096$. (g) $\kappa = 1.5$, $\Delta p = 0.00036$, $\lambda = -0.006$. (h) $\kappa = 5$, $\Delta p = 0.0012$, $\lambda = -0.0156$.

is assured to be valid, and in this case, a single polymer chain undergoes a mean field generated by the solvent monomers, membrane, and chain itself. Furthermore, in some cases, for example, when the interaction between rod segments and membrane can be ignored, the distribution of rod segment is spatially uniform, the density distribution of rod segment and thus the vesicle shape can be solved exactly without the SCFT. In our system, however, due to introduction of the interaction between rod and membrane, the spatial distribution of rod will not be uniform any more, and the rod segment except the anchor touches the membrane transiently, resulting in randomly dis-

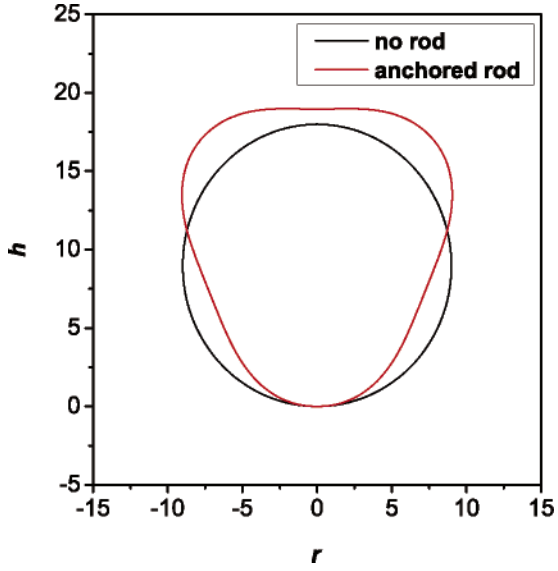

Figure 3. Transformation of vesicle shape after anchored rod. In all cases, we use $c_0 = 0$, $\chi = 0$, $\eta = 0$, $\kappa = 5$, $\Delta p = 0.0012$, $\lambda = -0.02698$. The rod length is $N_p = 100$.

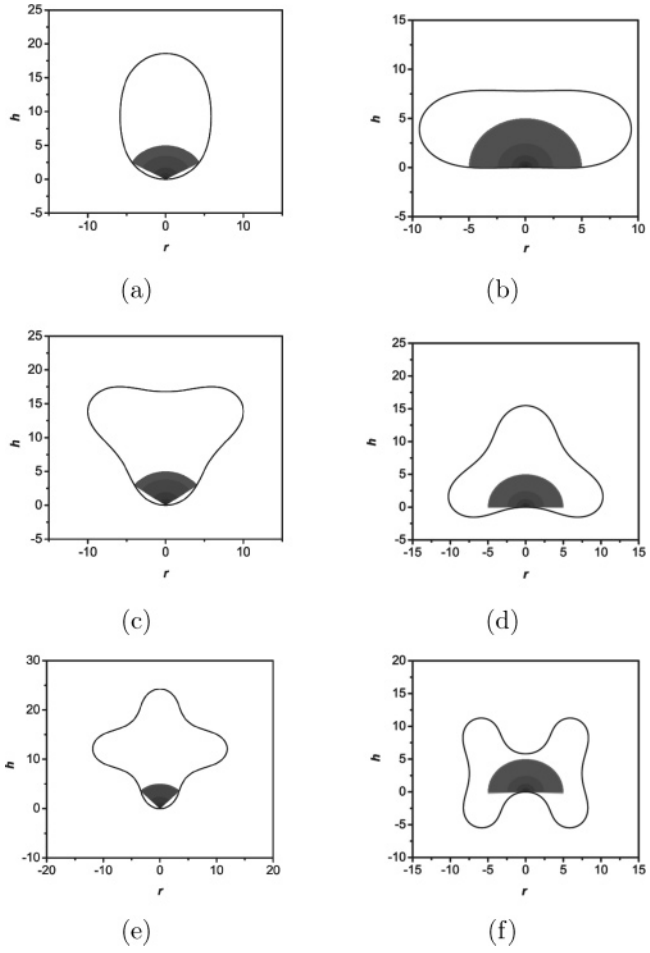

Figure 4. Typical stationary solutions of vesicle anchored by rigid rod inside, including shapes of the vesicle and segment distributions of the anchored rod. The shape of the vesicle is represented by the solid curve, and the density of the polymer chain is drawn in gray scale on a logarithmic scale. The radial (horizontal) and height axes are scaled by Nb. In all cases, we use $N_p = 100$, $c_0 = 0$, $\chi = 0$, $\eta = 0$. (a) $\kappa = 10$, $\Delta p = 0.0024$, $\lambda = -0.04$. (b) $\kappa = 15$, $\Delta p = 0.0036$, $\lambda = -0.06$. (c) $\kappa = 5$, $\Delta p = 0.0012$, $\lambda = -0.024$. (d) $\kappa = 10$, $\Delta p = 0.0024$, $\lambda = -0.036$. (e) $\kappa = 2$, $\Delta p = 0.00048$, $\lambda = -0.0096$. (f) $\kappa = 2$, $\Delta p = 0.00048$, $\lambda = -0.008$.

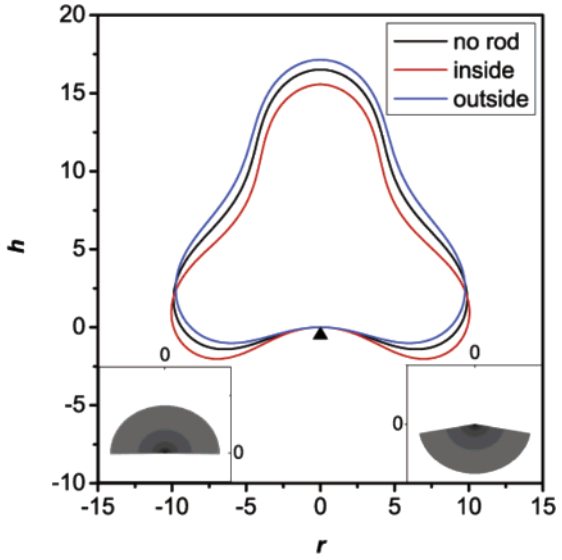

Figure 5. Shape of vesicle anchored by rigid rod outside ($\zeta > 0$) and inside ($\zeta < 0$). $N_p = 100$, $\kappa = 10.0$, $c_0 = 0$, $\Delta p = 0.0024$, $\chi = 0$, $\eta = 0$, and $\lambda \sim -0.045$ is set to keep the area of vesicle to be constant.

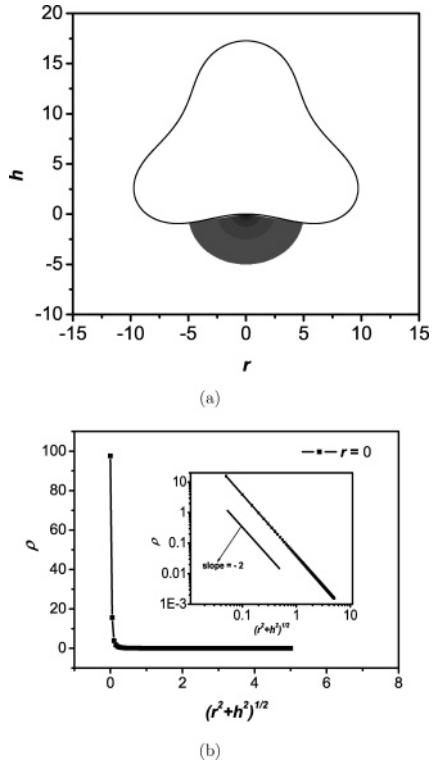

Figure 6. Shapes of the vesicle anchored by a rigid rod (a) $\kappa = 10.0$, $N_p = 100$, $c_0 = 0$, $\Delta p = 0.0024$, $\lambda = 0.004$, $\chi = 0$, $\eta = 0$. The density of the rigid rod is drawn in gray with the logarithmic scale. The shape of vesicle is represented by solid curves, and the axis are scaled by $N_p b$. (b) The density profile of the rod along the vertical directions ($r = 0$). In the inset, the density profiles are drawn in logarithm scale.

tributed touching point. Therefore, in this regard one of the efficient and popular techniques to obtain the probability distribution of rod segments is the self-consistent field method.

3. Results and Discussion

3.1. $\chi = 0$ and $\eta = 0$. The spherical vesicle are usually disturbed by temperature and osmotic pressure, and it can take various shapes. According to the index of spherical harmonic (l), $l = 1$ denotes spherical vesicle and $l = 2$ denotes that vesicles

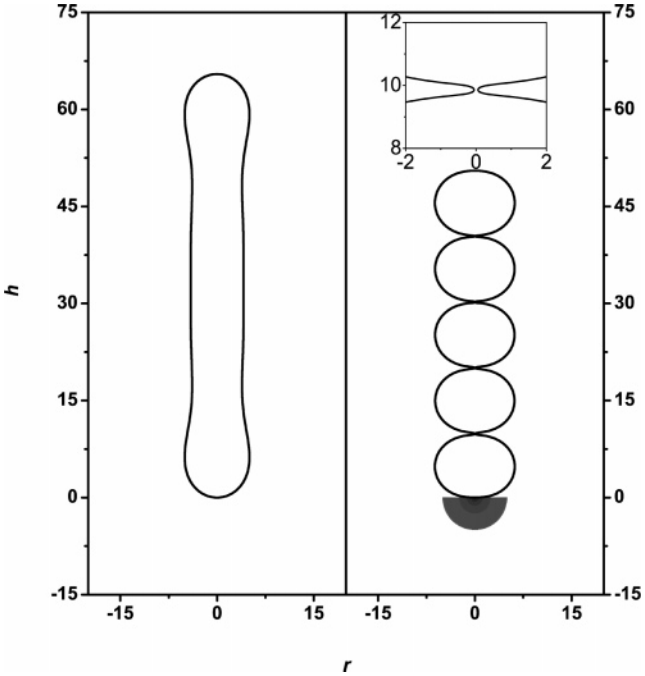

Figure 7. Pearling transition of tubular vesicles due to rod anchoring. The tubular vesicle shown in the left panel is obtained with parameters: $\kappa = 10$, $c_0 = 0$, $\chi = 0$, $\eta = 0$, $\Delta p = 0.0024$, $\lambda = -1.5(\Delta p/2)^{2/3}$. The pearling vesicle in the right panel is with the same parameters, but a rod with chain length $N_p = 100$ anchored. The inset depicts the pore between the bottom pearl and its neighbor.

have 2-fold symmetry, etc. Here, we should mention that, due to the disturbance of the anchored rod, the shapes usually cannot be described by a single index of spherical harmonics. Therefore, in the following we approximately label the shape by its dominate index of spherical harmonics (i.e., $l \sim 2$, $l \sim 3$, etc.). In principle, eq 14 has a complete set of solutions for given parameters (λ, ΔP, c_0, etc.). These solutions of shape eq 14 that are the stationary shapes of vesicle contain local minima or saddle points in the space of all shapes. In this part, we only investigate the simplest case $c_0 = 0$ without any interaction potential (i.e., $\eta = 0$ and $\chi = 0$). As shown in Figure 2, we can obtain various stationary shapes, for example, oblates, prolates, stomatocytes, and more complex shapes ($l \sim 3$, $l \sim 4$). Figure 3 shows the transformation of vesicle after anchored rod. Note that due to the local disturbing of the rod, the sphere becomes unstable and transforms to the shape of starfish. This behavior has been observed in the system of vesicle formed with SOPC when PEG-Flu-Chol solution was introduced.[27] For the other shapes ($l > 2$) of vesicle, their shapes are also adjusted accordingly due to the rod anchoring.

In the real biological systems, some proteins, such as peripheral proteins, could also exist inside the biological cell membranes. These proteins can affect the shape of biological membranes either. In this case, vesicle is deformed because the anchored rod segment exert the inhomogeneous entropic pressure on the inner side of membrane. As shown in Figure 4, there are various stationary shapes of vesicle also. Similar to the outside anchoring situation, the sphere vesicle becomes unstable and thus cannot be observed any more; other shapes ($l \gtrsim 2$) of vesicle are adjusted accordingly. The behavior of vesicle deformation is different for the same set of membrane parameters when the rod anchored outside and inside the vesicle. As shown in Figure 5, for the starfish shaped vesicle ($l \sim 3$), the vesicle shape is elongated along the axis of axial symmetry **h** and the membrane near the south pole is adjusted to be more

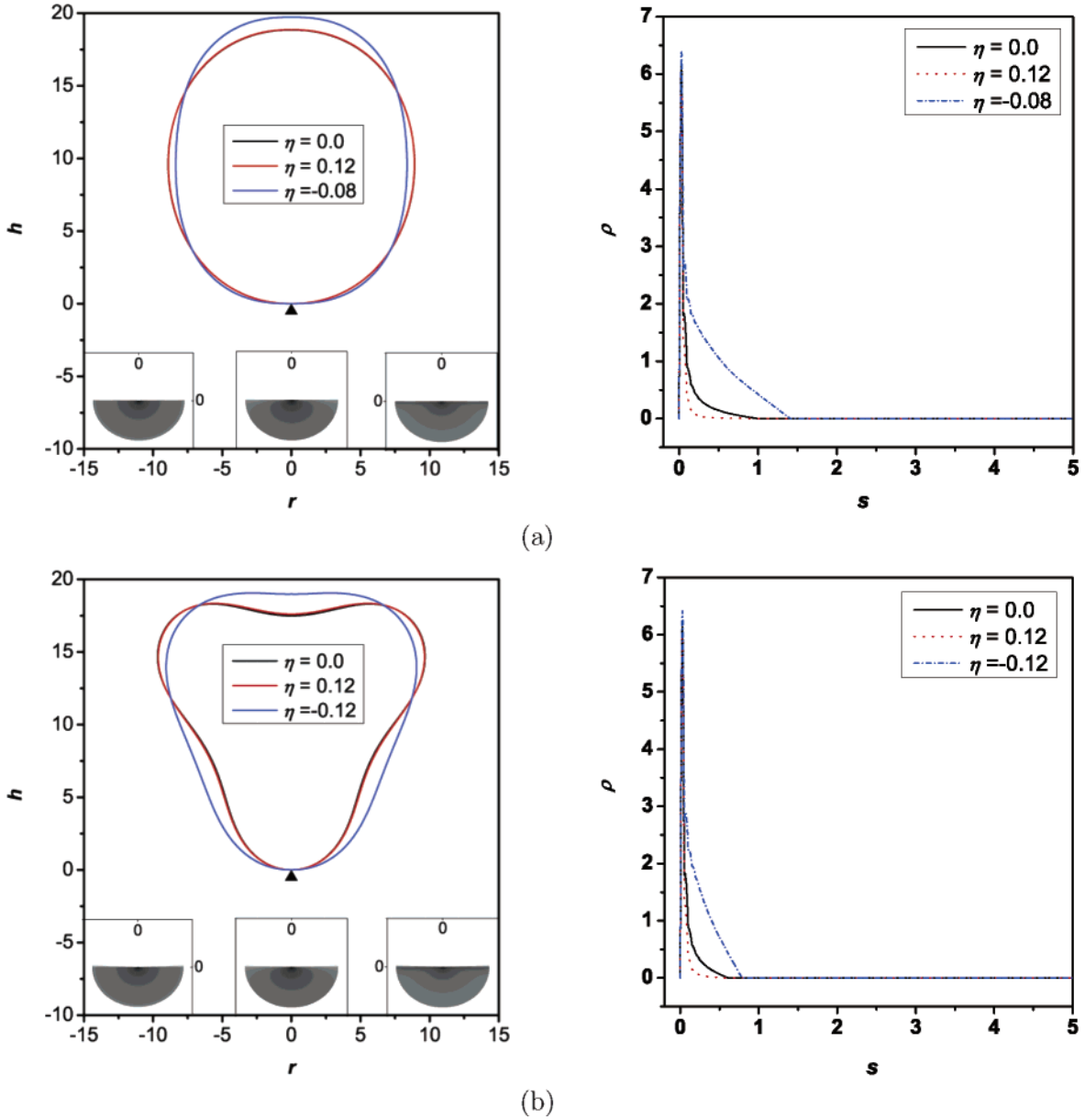

Figure 8. Shape of the vesicle anchored by the rigid rod for different interaction parameter η with $\kappa = 10.0$, $N_p = 100$, $c_0 = 0$, $\Delta p = 0.0024$, $\chi = 0$, and $\lambda \sim -0.05$ is set to keep the area of vesicle to be constant. The shape of the vesicle is represented by solid curves, and the density of the polymer chain is drawn in gray scale of its shape color map by logarithm scale. The density of rod on membrane near grafted point is drawn on the right side.

flat when rod is anchored outside. In contrast, the vesicle is elongated perpendicular to the axis of symmetry **h** and the membrane near the south pole become much more steep when the rod is anchored inside. The intrinsic reasons are that the vesicle membrane cannot be penetrated by the rod, and resulting in the inhomogeneous entropic pressure exerted on the membrane. The final shape of this system is the balance between the bending and tension energies of vesicle and the entropic pressure exerted by the rod. To achieve larger space and maximize the orientational entropy of rod, the vesicle is elongated along the axis of symmetry **h** when the rod is anchored outside. Due to the same reason, the vesicle is elongated perpendicular to the axis of symmetry **h** when the rod is anchored inside. No matter if the rod is anchored outside or inside, the rod anchoring exerts the perturbation at small length scales and induces local inhomogeneous entropic pressure; the shape of vesicle would adjust and adopt the state of lower energy.

Figure 6 shows the shapes of the rod-anchored vesicle and the density of rod segment for the case of $l \sim 3$. Since the size of the rigid rod ($R_p = N_p b$) is much larger than that of Gaussian chain ($R_p = \sqrt{N_p} b$) with the same chain length, the contact distance between the rod and the vesicle is also much longer. Due to the rigidity of the rod and the continuity of the vesicle curvature, there is an empty space where no rod segments can be found near the anchoring position, as shown in Figure 6. The density of rod segment contacted to the vesicle membrane is much lower than that of Gaussian chain-anchored vesicle. According to the scaling theory,[28] inhomogeneous pressure was mainly exerted on vesicle near the anchoring position due to highly localized conformation fluctuations of flexible polymers. However, in the case of rod anchoring, not all rod segments could have the opportunity to contact to the membrane and to exert the entropic pressure on it. As shown in Figure 6, the densities drop suddenly from the anchoring position and then decay smoothly further away. The density of the rod segments

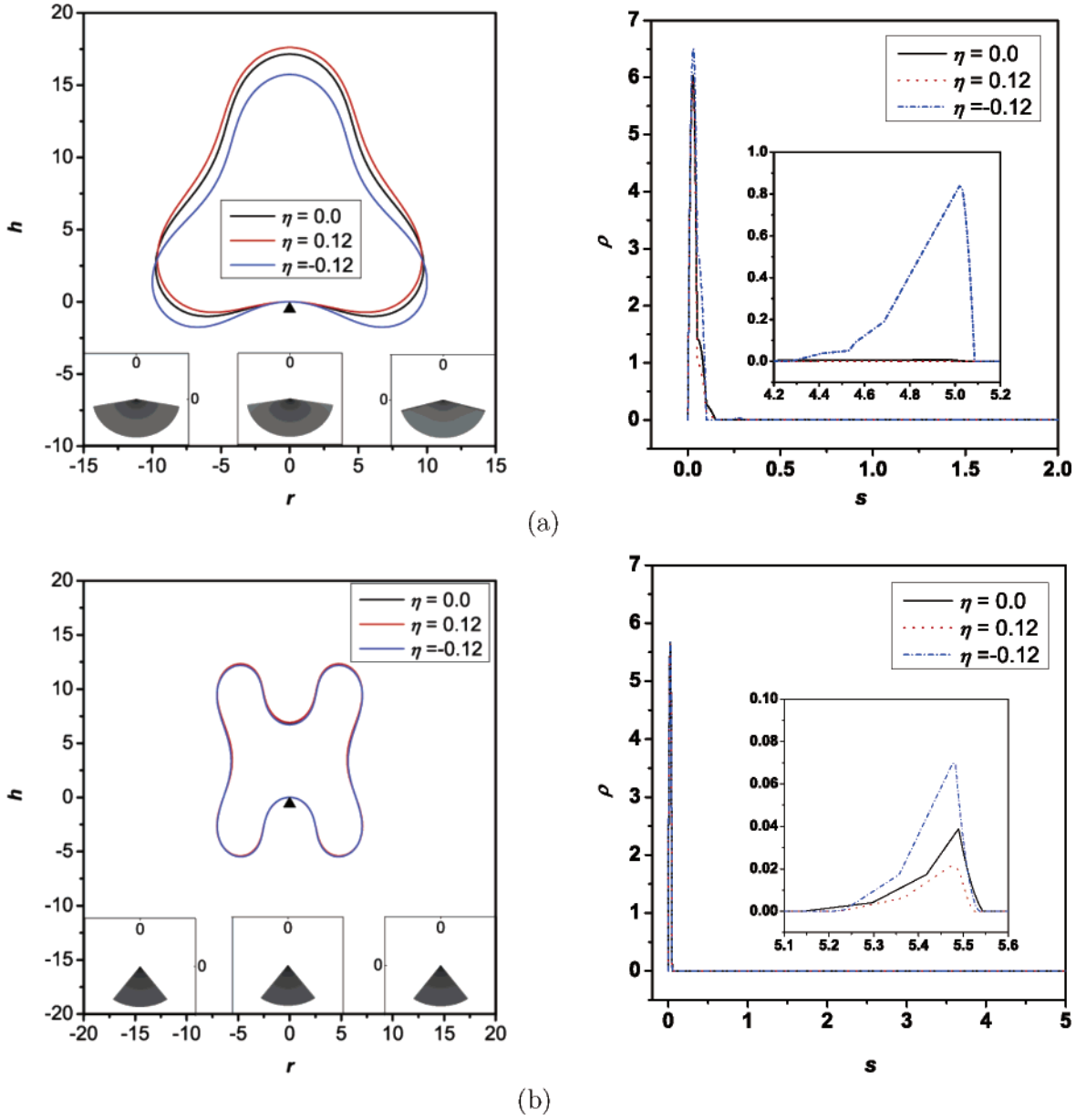

Figure 9. Shape of the vesicle anchored by the rigid rod for different interaction parameter η with $\kappa = 10.0$, $N_p = 100$, $c_0 = 0$, $\Delta p = 0.0024$, $\chi = 0$, and $\lambda \sim -0.05$ is set to keep the area of vesicle to be constant. The shape of the vesicle is represented by solid curves, and the density of the polymer chain is drawn in gray scale of its shape color map by logarithm scale. The density of rod on membrane near grafted point is drawn on the right side.

along the orientation of rod is shown in Figure 6b. Note that the density of rod segments is exponentially falling with the exponent of -2 from the anchoring position to the rod end. When there is no any interactions between the vesicle membrane and the rod, the density of rod segment meets the scaling behavior of

$$\rho(r, h) \propto \frac{1}{(r^2 + h^2)}, \quad (r^2 + h^2 < (N_p b)^2)$$

where r and h represent the space position in the cylinder coordinate system.

Tubular vesicle is common in nature, but it is not an stationary solution for the case of only considering the elastic energy.[29] When it is anchored by polymers, polymers will induce pearling instability.[17] Tsafrir et al.[4] have observed the pearling of vesicle formed with SOPC when dextran was introduced. In their opinion, the pearling instability is induced by the altering of the spontaneous curvature originated from the anchored polymer chain on the outer layer of the vesicle membrane. For a vesicle membrane with $c_0 = 0$ and $\lambda = -1.5(\Delta P/2)^{2/3}$, the vesicle can form an infinitively long tubular with radius $(\Delta P/2)^{-1/3}$.[24] Similar to experiments, if such a tubular vesicle is anchored by a rod with the same parameters, it becomes unstable and transforms to a shape comprising a chain of pearl with radius close to that of the original tubular, and each pearl is connected with its neighbor through a narrow pore, as shown in Figure 7. Because the spontaneous curvature is a constant ($c_0 = 0$) in calculation, the change of spontaneous curvature of vesicle may not be the only reason for pearling instability, and the inhomogeneous entropic pressure originated from the anchored rod segment is another plausible reason.

3.2. Effect of χ. The Flory−Huggins interaction parameter χ between the rod and the solvent does not explicitly appear in eq 14. However, the distribution of polymer segments will be affected by the quality of solvent, especially poor solvent.

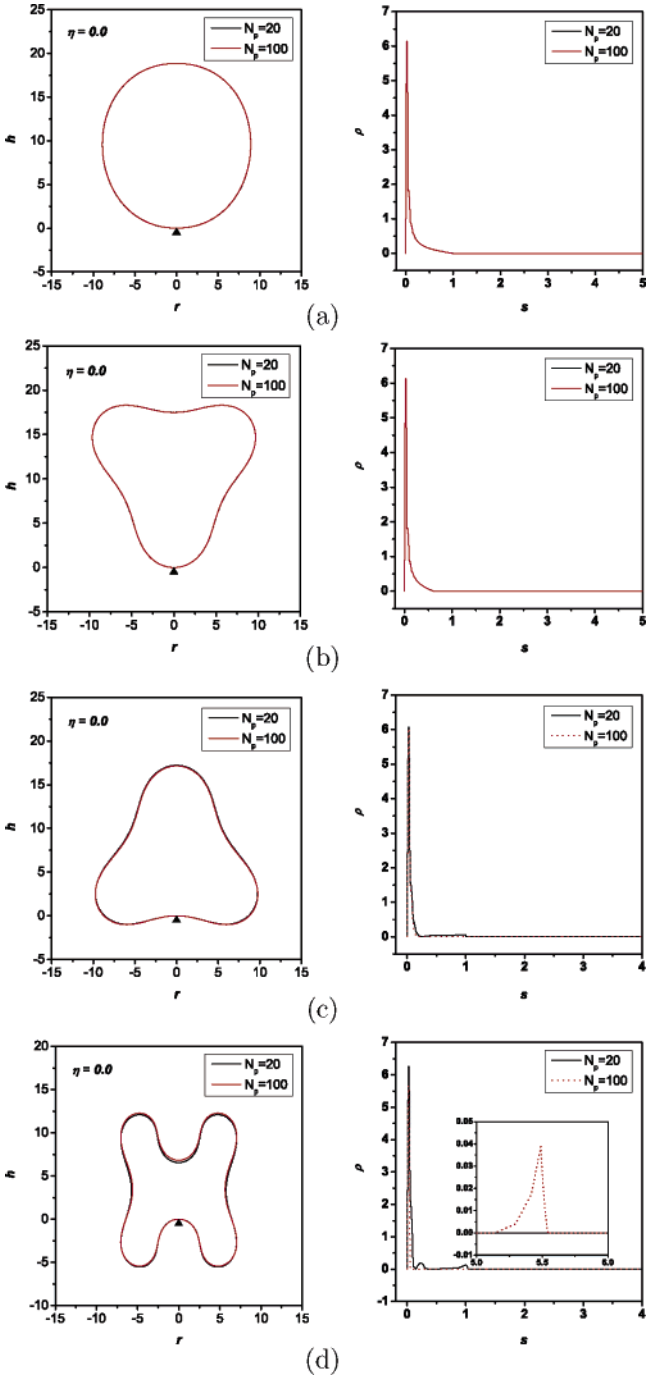

Figure 10. Shape of the rod-anchored vesicle for different rod length N_p with $\eta = 0$. $\kappa = 10.0$, $N = 100$, $c_0 = 0$, $\Delta p = 0.0024$, $\chi = 0$, and $\lambda \sim -0.05$ is set to keep the area of vesicle to be constant. The density of rod on membrane near grafted point is drawn on the right side.

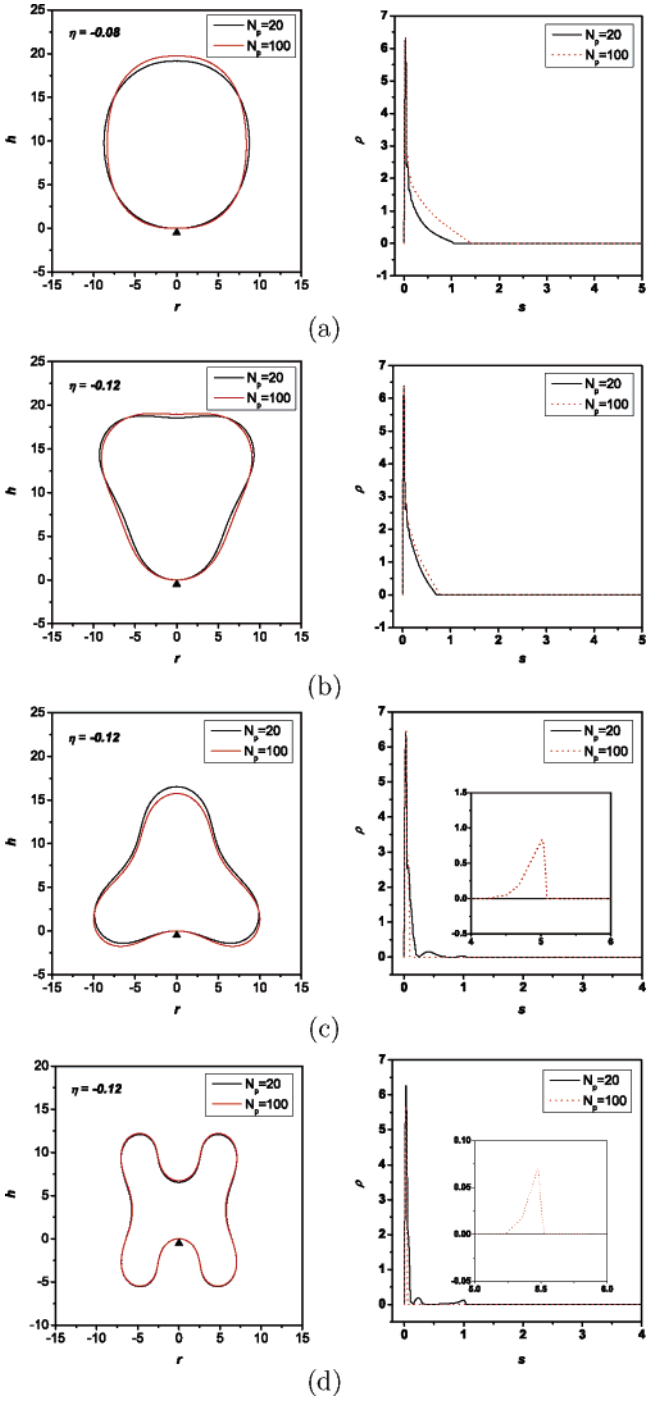

Figure 11. Shape of the rod-anchored vesicle for different rod length N_p with $\eta \neq 0$. $\kappa = 10.0$, $N = 100$, $c_0 = 0$, $\Delta p = 0.0024$, $\chi = 0$, and $\lambda \sim -0.05$ is set to keep the area of vesicle to be constant. The density of rod on membrane near grafted point is drawn on the right side.

Therefore, the interaction parameter implicitly changes the shape of vesicle through the distribution of chain segments. This has been verified for a Gaussian chain-anchored vesicle.[30] However, this effect is very small compared to other parameters. For the rod-anchored vesicle, this effect is even more insignificant since the rod is rigid and the distribution of the rod segment is almost not influenced within the reasonable range of χ. Indeed, increasing solvent−rod exclusive interaction causes a slight change of the vesicle shape because, in a bad solvent ($\chi > 0$), the rod prefers to stay close to the membrane. Different from the flexible chains, due to the rigidity of the rod, the quality of solvent barely affects the distribution of rod density, thus its effect on the shape of vesicle can be ignored.

3.3. Effect of η. The interaction between rod segment and membrane can be described by a Flory−Huggins type of parameter, η. In Figures 8 and 9, the shapes of the rod-anchored vesicle and the distribution of rod segments are presented for various interaction strength η. $\eta > 0$ and $\eta < 0$ denote the repulsion and adsorption interactions, respectively. In the following calculation, the surface area of the vesicle is kept constant. As shown in the insets of Figures 8 and 9, the distribution of rod segments is changed when the interaction between the rod and the membrane is switched on. The probabilities of the rod segments appearing near the vesicle membrane and the density of rod segment on the vesicle

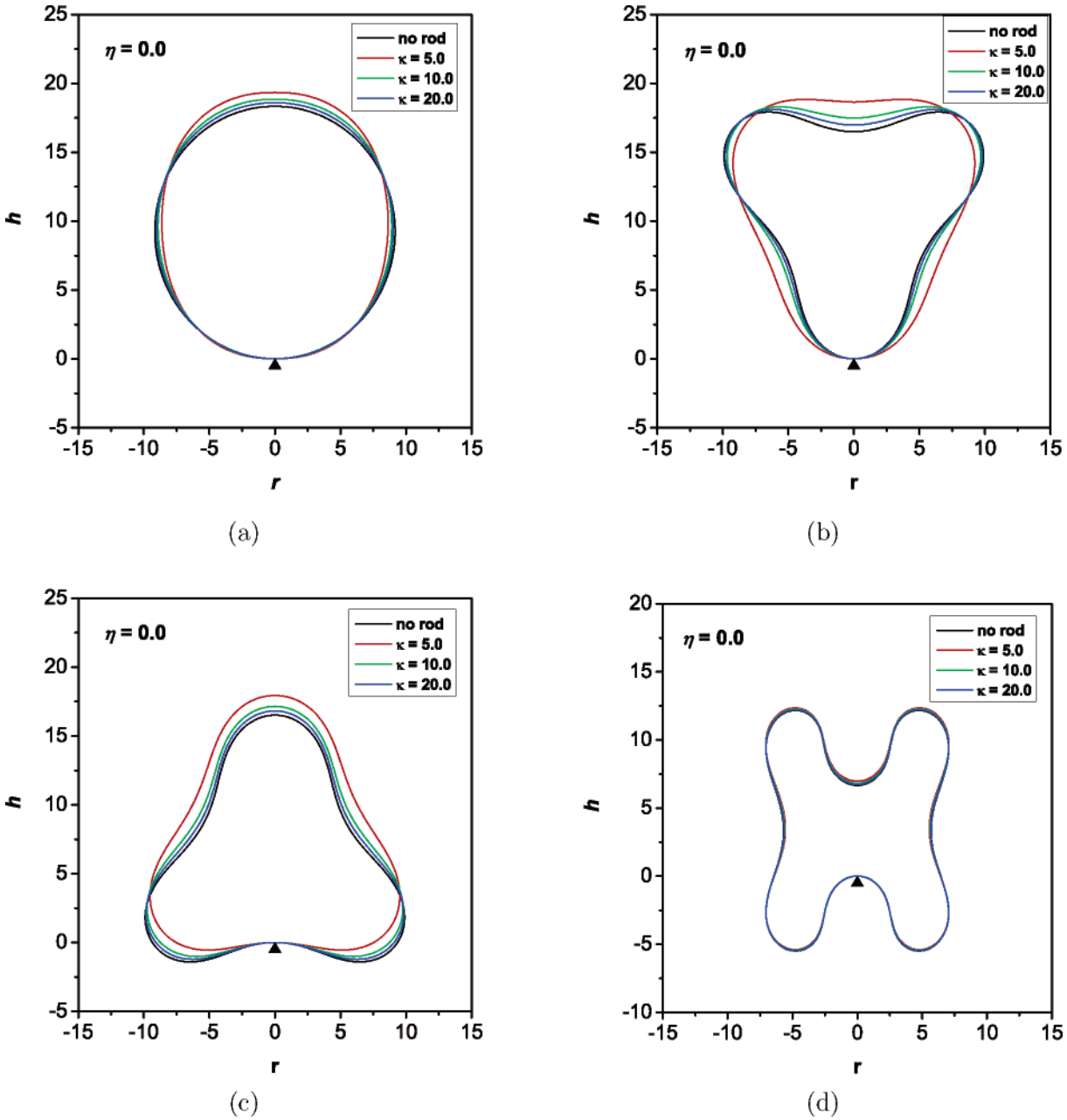

Figure 12. Shape of the rod-anchored vesicle for different bending rigidity κ. The parameters used are $N_p = 100$, $c_0 = 0$, $\Delta p = 0.0024$, $\chi = 0$, and $\lambda \sim -0.05$ is set to keep the area of vesicle to be constant.

membrane increase with decreasing η. Accordingly, the vesicles adjust its shape to minimize the free energy for the altered distribution of rod segments density when $\eta < 0$. When $\eta < 0$, the density of rod segment on the vesicle surface and the inhomogeneous entropic pressure $\zeta\rho_p(r \in A[\mathbf{R}_m])$ increase with adsorption strength $|\eta|$, and the shape of the vesicle changes remarkably. On the contrary, when $\eta > 0$, the shape of vesicle scarcely changes due to the reduction of $\rho_p(r \in A[\mathbf{R}_m])$. More interestingly, it is found that the effect of η is strongly dependent on the shape of vesicles (different l). For example, for the case of $l \sim 4$ shown in Figure 9b, both $\eta > 0$ and $\eta < 0$ only induce a very small shape deformation. This is due to the rigidity of the rod and the character of vesicle shape. For the case of $l \sim 4$, the segment density on the membrane, $\rho_p(r \in A[\mathbf{R}_m])$, is much lower than the cases of $l \sim 2$ or $l \sim 3$. This behavior is very different from the Gaussian chain-anchored vesicle.[17] Because of the rigidity of the rod and the continuity of the vesicle curvature, there is an empty space between vesicle and rod. Hence, the density of rod segments on the vesicle surface is much lower than Gaussian chains. Especially, the density near the anchored position decrease dramatically. One should notice that, for the case of $\eta < 0$, the inhomogeneous entropic pressure $\zeta\rho_p(r \in A[\mathbf{R}_m])$ increases and the extra tensile stress $\eta\rho_p(r \in A[\mathbf{R}_m])$ decreases with increasing $|\eta|$. In addition to that, the term of $\eta\mathbf{n}\cdot\nabla\rho(r \in A[\mathbf{R}_m])$ usually counteracts the inhomogeneous entopic pressure term $\zeta\rho_p(r \in A[\mathbf{R}_m])$ for rod-anchored vesicle. This is another key factor should be taken into account for the vesicle shape transformation.

3.4. Effect of Rod Length. The effect of rod length on the vesicle shapes are shown in Figures 10 and 11. In general, with increasing the rod length $N_p b$, the rod will exert the inhomogeneous entropic pressure to the vesicle in a larger area. However, as shown in Figure 10a−d ($l \sim 2, 3$), except for panel d ($l \sim 4$), the shape of vesicle is barely affected by the length of rod. It is clear that the effect of rod length is very small when the vesicle membrane near the anchoring point is convex.

In contrast to that when the vesicle membrane near the anchoring point is concave, such as $l \sim 4$, the orientational entropy is largerly reduced for longer rod; thus, the shape of vesicle will be influenced stronger.

However, the rod length will influence the shapes of rod-anchored vesicles even in the weak adsorption as shown in Figure 11a−d. The interactions between rod and membrane result in the redistribution of chain segments near the vesicle membrane. With the rod length increasing, the vesicle membrane near the anchored position is drawn close to the rod and deforms accordingly. Same as the situation of no interaction between rod and membrane, the shape deformation relys on the shape of vesicle, especially the local curvature near the anchoring position.

3.5. Effect of Bending Rigidity. The bending rigidity of vesicle is a kind of capability that can resist perturbation and deformation. For phospholipid membranes, one finds $\kappa = 10-40\ k_BT$,[25] which is high as compared to the thermal energy k_BT. The bending rigidity depends on the local heterogeneous concentration of the species, such as protein molecules on the blood cells.[31] As cytoskeleton, rigid macromolecules can increase more or less the bending rigidity and then restrain thermal fluctuations of membrane, as demonstrated by some experiments.[32] The effect of the bending rigidity of the vesicle without any interaction ($\eta = 0$) is shown in Figure 12. The deformation of vesicle increases gradually as the bending rigidity decreases from $\kappa = 20$ to $\kappa = 5$. Note that the vesicle with large bending rigidity can resist extra inhomogeneous entropic pressure due to the rod anchoring and only deform slightly.

4. Conclusion

A method combined the self-consistent field theory for rod with the Helfrich curvature elasticity theory for the membrane is developed for the rigid rod-anchored vesicles. Both density distribution of rod segments and deformation of the vesicle are obtained. It is found that due to the vesicle's impenetrability for the rod segments and the decrease of the available space for the rod orientational configuration, the anchored rod segment exerts the inhomogeneous entropic pressure on the vesicle, and the shape of vesicle is transformed. The behavior of vesicle deformation is different when the rod is anchored outside or inside of the vesicle. The vesicle is elongated along the axis of symmetry, and the membrane near the south pole transforms to be much more flat when the rod is anchored outside. The vesicle is elongated perpendicular to the axis of symmetry, and the membrane near the south pole becomes much more steep when the rod is anchored inside. When the interaction between the vesicle membrane and the rod segments is weak adsorption, the anchoring rod not only exerts the inhomogeneous entropic pressure on the vesicle but also changes the tension of membrane so that the deformation of vesicle is remarkable. High bending rigidity of the membrane can resist the extra inhomogeneous entropic pressure as well as the shape change of the vesicle. The length of rod barely affects the shape of vesicle at $\eta = 0$. However, when there are adsorptions between vesicle and rod, the effect of rod length is enhanced. In addition, the quality of the solvent scarcely influences the density distribution of rod segments and the shape of the vesicle due to the fact that the solvent will never alter the configuration of the rigid rod-like polymers. The results presented here can provide valuable insights into some biological process. Meanwhile, it is easy to extend this method to more complicated and real biological systems, such as polymers with different topological architectures/vesicle, multiple chains/vesicle, protein inclusions, etc.

Acknowledgment. We gratefully acknowledge financial support from the National Basic Research Program of China (Grant 2005CB623800) and the National Natural Science Foundation of China (Grants 20104002, 20234010, 20374016, 20304002, and the Grant for the Excellent Research Group). We thank Drs. Jiafang Wang, Kunkun Guo, and Jiajing Xu and Mr. Jianfeng Li for useful discussions.

References and Notes

(1) Lipowsky, R.; Sackmann, E. In *Structure and Dynamics of Membranes, Handbook of Biological Physics*; Elsevier: Amsterdam, 1995; Vol. 1.
(2) Alberts, B.; Bray, D.; Johnson, A.; Lewis, J.; Raff, M.; Roberts, K.; Walter, P. *Essential Cell Biology*; Garland Publishing: New York, London, 1998.
(3) Dobereiner, H. G.; Evans, E.; Krauss, M.; Seifert, U.; Wortis, M. *Phys. Rev. E* **1997**, *55*, 4458.
(4) Tsafrir, I.; Caspi, Y.; Arzi, T.; Stavans, J. *Phys. Rev. Lett.* **2003**, *91*, 138102.
(5) Blume, G.; Ceve, G. *Biochim. Biophys. Acta* **1990**, *1029*, 91.
(6) Lasic, D. D. *Angew. Chem., Int. Ed. Engl.* **1994**, *33*, 1685.
(7) Kim, Y. W.; Sung, W. *Phys. Rev. E* **2001**, *63*, 041910.
(8) Hiergeist, C.; Lipowsky, R. *J. Phys. II (France)* **1996**, *6*, 1465.
(9) Lipowsky, R. *Europhys. Lett.* **1995**, *30*, 197.
(10) Lipowsky, R.; Doebereiner, H. G.; Hiergiest, C.; Indrani, V. *Physica A* **1998**, *249*, 536.
(11) Brooks, J.; Margues, C.; Cates, M. *J. Phys. II (France)* **1991**, *1*, 673.
(12) Breidenich, M.; Netz, R. R.; Lipowsky, R. *Europhys. Lett.* **2000**, *49*, 431.
(13) Kim, Y. W.; Sung, W. *Phys. Rev. E* **2001**, *63*, 041910.
(14) Bickel, T.; Jeppesen, C.; Marques, C. M. *Phys. Rev. E* **2000**, *62*, 1124.
(15) Bickel, T.; Jeppesen, C.; Marques, C. M. *Eur. Phys. J. E* **2001**, *4*, 33.
(16) Bickel, T.; Marques, C. M. *Eur. Phys. J. E* **2002**, *9*, 349.
(17) Wang, J. F.; Guo, K. K.; Qiu, F.; Zhang, H. D.; Yang, Y. L. *Phys. Rev. E* **2005**, *71*, 041908.
(18) Guo, K. K.; Qiu, F.; Zhang, H. D.; Yang, Y. L. *J. Chem. Phys.* **2005**, *123*, 074906.
(19) Doi, M.; Edwards, S. F. *The Theory of Polymer Dynamics*; Clarendon Press: Oxford, 1986.
(20) Ariel, G.; Andelman, D. *Phys. Rev. E* **2003**, *67*, 011805.
(21) Ou-Yang, Z. C.; Helfrich, W. *Phys. Rev. Lett.* **1987**, *59*, 2486.
(22) Matsen, M. W.; Schick, M. *Phys. Rev. Lett.* **1994**, *72*, 2660.
(23) Ou-Yang, Z. C.; Liu, J. X.; Xie, Y. Z. *Geometric Methods in the Elastic Theory of Membranes in Liquid Crystal Phases*; World Scientific Press: Singapore, 1999.
(24) Seifert, U.; Berndl, K.; Lipowsky, R. *Phys. Rev. A* **1991**, *44*, 1182.
(25) Bar-Ziv, R.; Moses, E. *Phys. Rev. Lett.* **1994**, *73*, 1392.
(26) Evans, E.; Rawicz, W. *Phys. Rev. Lett.* **1997**, *79*, 2379.
(27) Dobereiner, H. G.; Lehmann, A.; Goedel, W.; Selchow, O.; Lipowsky, R. *Mater. Res. Soc. Symp. Proc.* **1998**, *489*, 101.
(28) de Gennes, P. G. *J. Phys. Chem.* **1990**, *94*, 8407.
(29) Harbich, W.; Deuling, H. J.; Helfrich, W. *J. Phys. (France)* **1977**, *38*, 727.
(30) Guo, K. K.; Qiu, F.; Zhang, H. D.; Yang, Y. L. *Acta Phys. Sinica* **2006**, *55*, 155.
(31) Du, Q.; Liu, C.; Wang, X. Q. *J. Comput. Phys.* **2004**, *198*, 450.
(32) Gov, N.; Zilman, A. G.; Safran, S. *Phys. Rev. Lett.* **2003**, *90*, 228101.